Surface-plasmon energy gaps and photoluminescence

S. C. Kitson, W. L. Barnes, and J. R. Sambles
Department of Physics, University of Exeter, Stocker Road, Exeter EX4 4QL, United Kingdom
(Received 17 March 1995)

Excited dye molecules on a metallic grating can relax by generating surface plasmon polaritons (SPP's). These SPP's can scatter from the grating reradiating their energy as photons. For dye molecules in contact with the metal, light radiated by SPP's dominates the optical emission from the system. If the wavelength of the SPP is equal to half the pitch of the grating then the mode can Bragg reflect from the surface and an energy gap opens up in the SPP dispersion. This paper examines the effect that such an energy gap has on the emission properties of the dye. Experimentally it is found that the SPP energy gap significantly inhibits emission from the system. Numerical modeling is used to show that the modified emission spectrum is determined by the wavelength dependence of the density of available SPP states.

I. INTRODUCTION

There is much current interest in the interaction between electromagnetic radiation and materials that are periodic on the scale of the wavelength of light (see, for example, Ref. 1). In much the same way that energy gaps occur for electrons propagating in periodic crystalline structures, the interaction between light and the material can lead to energy gaps for modes propagating in such media.[2,3] These photonic gaps offer the prospect of being able to modify the optical properties of systems by appropriate design of the material structure. In particular, the potential control of spontaneous emission is of considerable interest.[4,5] This paper considers how an energy gap for surface-plasmon polaritons (SPP's) propagating on a metallic grating can be used to modify the emission properties of an adjacent thin dye layer.

Dye molecules placed close to metal surfaces couple strongly to surface plasmon polaritons (SPP's). If the surface is planar then these modes cannot reradiate their energy as photons and the energy is ultimately lost as heat to the metal. If, however, the surface is corrugated then the SPP's can scatter from the surface and couple to photons, resulting in optical emission in well-defined directions and with a characteristic polarization.

If the pitch of the corrugation is appropriate then the SPP's can Bragg reflect and an energy gap opens up in the dispersion of the mode. If this gap coincides with the emission spectrum of the molecule then the SPP decay channel is blocked. This paper describes the effect of the gap on the emission properties of the system. In particular it is found that emission is significantly inhibited in the vicinity of the gap, and that the modified emission spectrum is determined by the wavelength dependence of the density of SPP states.

Figure 1 illustrates the sample geometry; a thin layer of laser dye (DCM) was deposited onto the surface of a silver grating. Excited dye molecules can relax by generating SPP's that propagate at the metal/dye interface. These nonradiative modes are *p*- (TM) polarized and can scatter from the grating and couple to photons.[6–8] The light is emitted in well-defined directions and has a characteristic polarization. This paper considers only the emission in the plane normal to the surface and to the grating grooves. In this case, the light reradiated by SPP's is *p*-polarized and is emitted at an angle θ such that

$$k_0 \sin\theta = \pm k_{\mathrm{SPP}} \pm nG \ , \tag{1}$$

where k_0 is the wave vector of the emitted light, k_{SPP} is the wave vector of the SPP, n is an integer and G is the grating vector (equal to 2π/grating pitch). Equation (1) is derived by requiring that the momentum of the SPP matches the component of the photon wave vector in the plane of the grating.[9]

Figure 2 shows an experimental measurement of the emission from a thin dye layer on a silver grating. The *p*-polarized emission is dominated by two strong peaks, at 13.1° and 35.2°. These peaks arise from the scattering of SPP's from the grating. The strongest peak is due to first-order scattering ($n=1$) and the weaker peak is produced by second-order scattering ($n=2$). The *s*-polarized emission shows no such resonant features.

The excitation of SPP's is just one of a number of possible nonradiative routes by which the energy of the dye

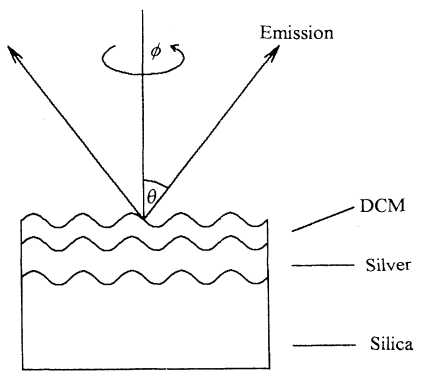

FIG. 1. Sample geometry.

0163-1829/95/52(15)/11441(5)/$06.00

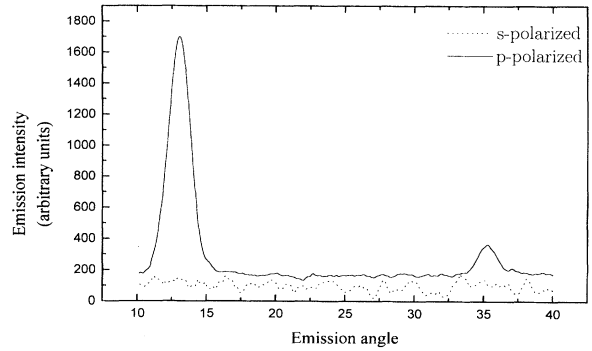

FIG. 2. The radiation pattern from a thin DCM layer on a silver grating with a pitch of 820 nm. Both *p*- and *s*-polarized emission are shown.

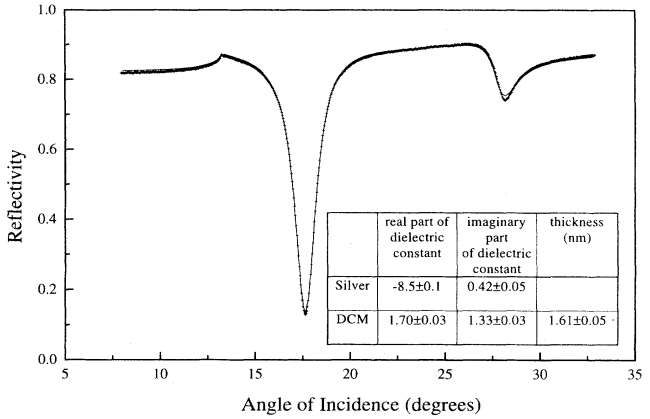

FIG. 3. The fitted reflectivity curve for the coated sample for 488 nm. The crosses are data, the line is the theoretical fit.

molecules can be absorbed by the metal. These include the excitation of electron-hole pairs and resistive damping, that is the conversion of electronic currents in the metal, induced by the near field of the molecule, into heat.[10] For an uncorrugated system all the energy nonradiatively transferred to the metal is ultimately lost as heat and the emission from the sample is strongly quenched. By corrugating the system, however, the energy transferred to SPP's can be recovered as photons. From Fig. 2 it is clear that, in this case, the emission is dominated by radiation from the SPP's; direct radiation is strongly quenched by the metal and is an order of magnitude less intense than the light reradiated via the first-order coupled SPP.

If the SPP wave vector is equal to half the grating vector then the SPP can Bragg reflect from the grating surface resulting in an energy gap in the dispersion of the mode.[11–15] By suitable choice of grating pitch the SPP energy gap can be made to coincide with the emission spectrum of the dye, blocking decay via SPP modes. In this case it is likely that the energy of the dye molecules will instead be lost via other nonradiative routes rather than direct emission, thus modifying the emission spectrum of the system. This paper presents an experimental investigation of the emission properties of such a system and shows that the emission spectrum is determined by the wavelength dependence of the density of available SPP states.

II. EXPERIMENT

The grating profile was holographically produced in a photoresist layer deposited on a silica substrate and transferred to the silica surface by etching with a beam of argon atoms in a high vacuum chamber. An optically thick silver film was then evaporated onto the surface of the grating. A thin layer of the laser dye DCM was subsequently deposited by spin deposition from a solution of the dye in methanol. A solution concentration of 0.4 mg ml^{-1} was used and the substrate spun at 3000 rpm.

The sample was characterized by measuring the angle-dependent reflectivity at 488 nm. When the angle of incidence θ satisfies Eq. (1), a *p*-polarized incident beam can resonantly excite SPP's, energy is absorbed from the beam, and the reflectivity is reduced. Fitting multilayer grating theory[16,17] to the data yields the optical constants of the layers and the profile of the grating surface.[18] Reflectivity data were recorded both before and after coating the silver grating with DCM. Fitting the data for the bare silver gave the silver parameters and the grating profile. These values were then fixed and the DCM parameters adjusted to obtain a good fit to the data for the dye-coated grating. A starting point for the DCM parameters was obtained by using the critical edge technique[21,22] to characterize a DCM layer on a bare prism. Figure 3 shows the data for the dye-coated grating, the fit, and the fitted optical constants.

The grating profile is described as a sum of harmonic components:

$$y(x)=d_1\sin Gx+d_2\sin(2Gx+\phi_2)\ . \tag{2}$$

Fitting theory to the reflectivity data for this grating gives pitch $=633.5\pm0.5$ nm, $d_1=17.3\pm0.5$ nm, $d_2=2.8\pm0.1$ nm, and $\phi_2=-90°$. The extra harmonic components arise from nonlinearities in the response of the photoresist during exposure in the interferometer. Generally only the first two or three components are significant.

The experimental measurements of the emission properties of the system consisted of recording the emission intensity as a function of the wavelength, the direction and the polarization of the emission. The sample was mounted in a holder that allowed the azimuthal angle of the sample to be set to a precision of $\pm0.5°$. The dye layer was excited by 488-nm emission from a 1-W argon ion laser made incident on the sample via a multimode optical fiber. The fiber was attached to the sample holder via a mount that included a graded index rod lens to focus the light onto the sample. In this way the argon ion beam moved with the sample as it was rotated during data acquisition, thus holding the angle of incidence and polarization of the incident beam fixed.

The sample holder was fixed to a computer controlled

rotating table to allow the angle of emission to be scanned. A lens collected the emission and focused it onto the slits of a spectrometer, the collection angle being limited to 1.5° by an aperture. The argon ion laser beam used to excite the dye layer was mechanically chopped at about 900 Hz so that phase-sensitive detectors could be used to record the signal from a photomultiplier situated at the exit slits of the spectrometer. A Glan-Thomson polarizer placed in front of the spectrometer selected either the *p*-polarized or the *s*-polarized component of the emission. A filter on the entrance slits prevented laser emission reaching the detector.

The wavelength resolution of the system was limited by the collection angle used. In practice a compromise had to be made between having acceptable wavelength and angle resolutions, and collecting enough light to ensure a reasonable signal level. Generally the angle resolution was ±0.8° and the wavelength resolution was ±5 nm.

III. RESULTS AND DISCUSSION

The angular positions of the emission peaks is related to the wave vector of the SPP's from which they originate [Eq. (1)]. Using the results from emission data, therefore, the dispersion curve for the mode can be constructed. In order to accurately determine the dispersion curve in the vicinity of an energy gap, data have to be recorded as a function of emission wavelength for fixed emission angles.[14,19] The peaks that occur in such data can then be accurately interpreted as corresponding to the resonant coupling between SPP's and photons. The finite width of the SPP resonance leads to misleading results if, instead, the peaks recorded in angle scans of the emission are used. Figure 4 shows an example of the emission data recorded as a function of the wavelength for emission normal to the sample.

The observed emission peaks arise from SPP's scattering from the fundamental (G) component of the grating surface. Light emitted normal to the sample arises from SPP's whose wave vector is equal to G [Eq. (1)]. Such modes, propagating in the direction of the grating vector, can Bragg reflect from the $2G$ component of the surface profile and form a standing wave. There are two possible

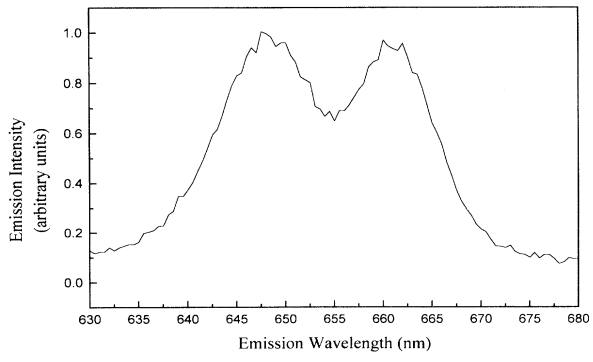

FIG. 4. Experimental emission data for emission normal to the sample. The two peaks correspond to the modes on either side of the energy gap.

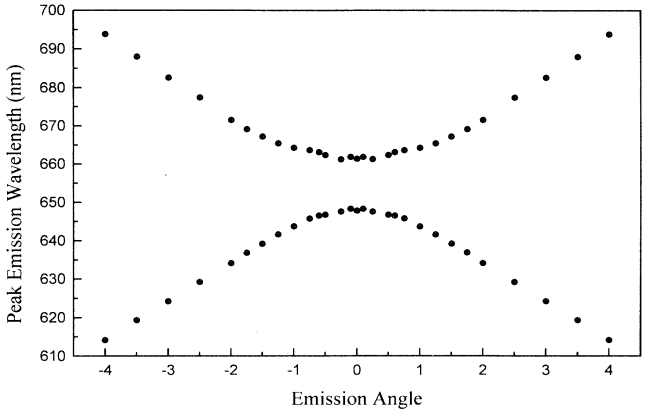

FIG. 5. The SPP dispersion curve constructed from measurements of the peak emission wavelength as a function of emission angle. There is a clear energy gap in the dispersion curve.

standing waves and it can be shown that these have different energies.[15] As a result an energy gap opens up in the dispersion of the mode, the width of which is linearly related to d_2, the amplitude of the $2G$ component. The standing waves can also be produced by Bragg reflection from the G component. This is, however, a second-order process and in practice has a negligible effect on the energy gap.

The two peaks in Fig. 4 therefore correspond to the modes on either side of the energy gap; the separation between the two gives the gap width, and the mean value corresponds to the central frequency of the gap. The positions of the peaks in such data were measured by fitting Gaussians to the emission curves.

The results of a series of emission measurements are shown in Fig. 5 where the peak emission wavelength is plotted as a function of the emission angle, this corresponds to the dispersion curve for the system. Data were only recorded for emission angles in the range 0° to 4°, but for clarity is shown for negative angles as well. This shows clearly that there is a 13.5±0.5-nm-wide gap centered at an emission wavelength of 654.5±0.5 nm.

For wavelengths within the gap there is no available SPP mode for the molecules to couple to so that this decay route is effectively blocked over this wavelength range. However, it has been shown[10] that, for molecules very close to a metal, decay via the excitation of electron-hole pairs and resistive damping are also strong decay channels. Removal of the SPP channel will, therefore, probably result in the energy being transferred to the metal via one of these alternative nonradiative routes rather than being emitted as a photon. Consequently the energy will not be radiated and one might expect that the photoluminescence in this wavelength range will be inhibited.

The spectrum of the light emitted in the plane normal to the grating grooves can be obtained by measuring the total intensity emitted at each wavelength. This can be achieved by recording the intensity as a function of emission angle for each wavelength; the area under the curve

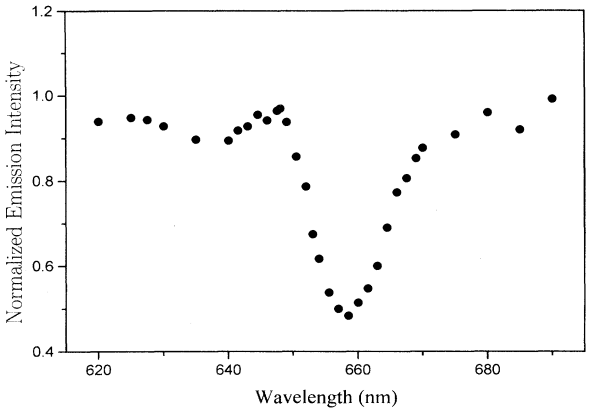

FIG. 6. The normalized emission spectrum for the sample exhibiting an energy gap, obtained by dividing the spectrum for the sample exhibiting a gap by that for a sample without a gap.

is proportional to the intensity emitted at that wavelength. Figure 6 shows such a spectrum for the sample exhibiting the gap. In order to take account of the intrinsic emission spectrum of the dye material the results have been normalized by dividing by the emission spectrum for a sample without an energy gap near the emission spectrum of the dye.

From Fig. 6 it is clear that there are several features that require explanation. Firstly, in the vicinity of the gap the emission is reduced by a factor of 2, but it is not completely inhibited. The curve is also asymmetric with a small dip in the emission intensity at about 638 nm. These features arise from the finite width of the SPP resonance and the nature of the mode dispersion and can be appreciated by considering a plot of the reflectivity response of the system, Fig. 7.

The emission spectrum was constructed by measuring the intensity as a function of emission angle for each wavelength and calculating the area under the peaks. As yet we cannot numerically model the emission from these structures, but one would expect to see similar behavior to that shown in the reflectivity response. Instead of reflectivity minima one would observe emission peaks but they should have similar widths and will follow the same dispersion curve.

Figure 7 is a theoretically generated reflectivity map for the sample and shows the reflectivity as a function of the wavelength and the angle of incidence. The parameters for the grating profile and DCM layer thickness were taken from the fit in Fig. 3. The values of the optical constants of the layers were fixed to those found at 664 nm.

Figure 7 shows clearly the presence of the gap and that the gap width is comparable to the width of the SPP resonance. It is also apparent that, at the edge of the gap, the low-energy branch cannot couple to photons. This is a consequence of the shape of the grating profile. The difference in the coupling strengths to the two branches can be explained in terms of the symmetry of the surface.[20]

In Fig. 4 the two modes give rise to equal strengths of emission because of the intrinsic emission spectrum of the dye. The dye emits far more strongly at 661 nm than at 647 nm. The difference in emission strength almost exactly compensates for the difference in coupling strength. Also, the collection angle of the detection equipment was substantially larger than the gap in the coupling strength to the low-energy branch.

Figure 8 shows the result of taking slices through the reflectivity map at constant wavelength and integrating the area of the reflectivity dips. These areas should exhibit the same behavior as those obtained by integrating the emission curves. The plot shows many of the same features as the spectrum of Fig. 6.

The area does not fall to zero in the center of the gap because the width of the SPP resonance is comparable to the gap width. It is clear from Fig. 7 that although there is no resonant coupling to a mode at the center of the gap, the wings of the modes on either side of the gap do overlap at that point. There is thus weak coupling between the SPP's and photons.

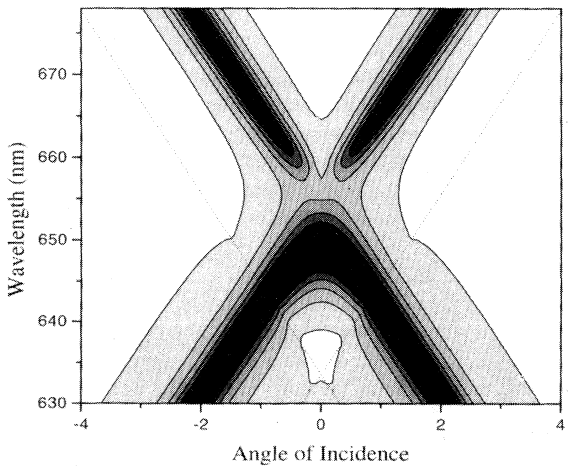

FIG. 7. Calculated reflectivity map for the grating exhibiting the energy gap. The dark regions correspond to low reflectivity, the light areas are high reflectivity. The dotted lines are the light lines representing the first order diffracted beams (see text).

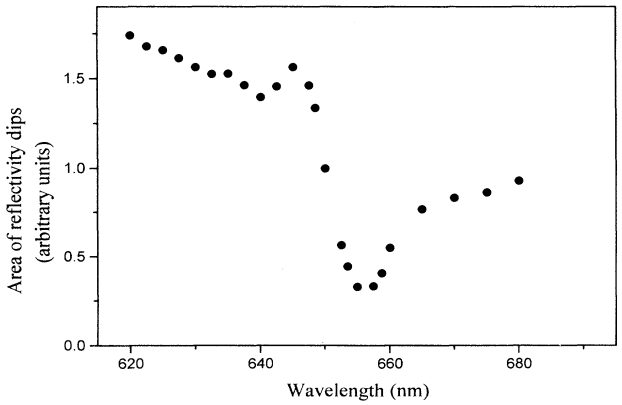

FIG. 8. The area of the reflectivity dips for slices taken at constant wavelength through Fig. 7.

The dip at 638 nm appears to be a consequence of the coupling between the SPP's and the first-order diffracted beams. The dotted lines in Fig. 7 represent the light lines that correspond to the plus and minus first-order diffracted beams. Points on these lines represent diffracted beams grazing along the surface of the grating. Points lying below these lines (that is to the low-wavelength side) correspond to diffracted beams propagating at less grazing angles; above the lines (to the high-wavelength side) the modes become evanescent and so do not propagate. The portions of the SPP dispersion curve that lie below the light lines can couple to the diffracted modes, providing a strong radiative decay channel for the SPP mode. This radiative loss contributes to the damping of the mode, which determines the width of the resonance.

When the light lines cross the dispersion curve the diffracted beams become evanescent, removing this radiative channel. The primary consequence of this reduction in damping of the mode is to reduce the width of the resonance; the depth of the resonance is also affected but to a lesser extent. The net result is a reduction in the area enclosed by the resonance that occurs as the wavelength rises to about 635 nm (Fig. 6). As the wavelength is increased further, and the edge of the gap approached, the dispersion curve becomes flattened. An angle scan at this wavelength (about 647 nm) actually runs along the dispersion curve for part of the way. The resonance will therefore appear to have a much larger width at this wavelength. This would seem to be the origin of the increase in the area under the resonance at the low-wavelength edge of the energy gap.

The areas plotted in Fig. 8 are related to the density of SPP states that are available at a particular wavelength. The energy gap modifies the emission spectrum by distorting the density of available states that can couple to light of a given wavelength. In the center of the gap there is no resonant coupling and the emission intensity drops, at the low-wavelength band edge there is a higher density of states due to the flattening of the dispersion curve, and there is a peak in the emission intensity. This feature is not seen on the high-wavelength side because the coupling strength drops to zero at the edge of the gap for this branch.

The agreement between Figs. 8 and 6 is not perfect, in particular there is a slope to the theory curve that is not present on the experimental data. Taking account of the wavelength dependence of the dielectric constants of the system may improve this. A full treatment would also have to take account of the finite resolution of the detection system.

IV. CONCLUSIONS

In this paper we examined experimentally the effect of an SPP energy gap on the emission from a dye layer adsorbed onto the surface of a metallic grating. Emission from this system is dominated by the reradiation from SPP's excited by the dye molecules. An SPP energy gap can block this decay channel and significantly inhibit the emission from the sample. We examined emission in the plane normal to the grating grooves and showed that the measured emission spectrum is determined by the wavelength dependence of the density of available SPP states. Since the width and central frequency of the energy gap depend on the nature of the surface profile[15] the emission properties of this system can be significantly modified by appropriate design of the surface morphology.

This paper has considered the effect of the SPP energy gap on the emission in the plane orthogonal to the grating grooves. Further work is being undertaken to investigate how the gap affects the emission in other directions[23] and the effect it has on the decay kinetics. Further work is also needed to develop a theoretical model to treat the emission from corrugated systems.

ACKNOWLEDGMENTS

The authors are grateful to the EPSRC and the DRA (Malvern) for supporting this research including the provision of a CASE award.

[1]J. Opt. Soc. Am. B **10**, No. 2 (1993).
[2]E. Yablonovitch, Phys. Rev. Lett. **58**, 2059 (1987).
[3]S. John, Phys. Rev. Lett. **58**, 2486 (1987).
[4]J. Martorell and N. M. Lawandy, Phys. Rev. Lett. **65**, 1877 (1990).
[5]E. Yablonovitch, J. Opt. Soc. Am. B **10**, 283 (1993).
[6]R. W. Gruhlke, W. R. Holland, and D. G. Hall, Phys. Rev. Lett. **56**, 2838 (1986).
[7]R. W. Gruhlke and D. G. Hall, Phys. Rev. B **40**, 5367 (1989).
[8]D. Heitmann, N. Kroo, C. Schulz, and Zs. Szentirmay, Phys. Rev. B **35**, 2660 (1987).
[9]H. Raether, *Surface Plasmons* (Springer-Verlag, Berlin, 1988).
[10]I. Pockrand, A. Brillante, and D. Mobius, Chem. Phys. Lett. **69**, 499 (1980).
[11]R. H. Ritchie, E. T. Arakawa, and J. J. Cowan, Phys. Rev. Lett. **21**, 1530 (1968).
[12]N. Kroo, Zs. Szentirmay, and J. Felszerfalvi, Phys. Lett. **86A**, 445 (1981).
[13]Y. J. Chen, E. S. Koteles, and R. J. Seymour, Solid State Commun. **46**, 95 (1983).
[14]D. Heitmann, N. Kroo, and C. Schulz, Phys. Rev. B **35**, 2660 (1987).
[15]W. L. Barnes, T. W. Priest, S. C. Kitson, J. R. Sambles, N. P. K. Cotter, and D. J. Nash, Phys. Rev. B **51**, 11 164 (1995).
[16]J. Chandezon, M. T. Dupuis, G. Cornet, and D. Maystre, J. Opt. Soc. Am. **72**, 839 (1982).
[17]N. P. K. Cotter, T. W. Priest, and J. R. Sambles, J. Opt. Soc. Am. **12**, 1097 (1995).
[18]E. L. Wood, J. R. Sambles, N. P. K. Cotter, and S. C. Kitson, J. Mod. Opt. **41**, 1343 (1995).
[19]M. G. Weber and D. L. Mills, Phys. Rev. B **34**, 2893 (1986).
[20]M. G. Weber and D. L. Mills, Phys. Rev. B **31**, 2510 (1985).
[21]F. Yang, J. R. Sambles, and G. W. Bradberry, J. Mod. Opt. **38**, 1441 (1991).
[22]S. C. Kitson and J. R. Sambles, Thin Solid Films **229**, 128 (1993).
[23]S. C. Kitson, Ph.D. thesis, 1995, University of Exeter, UK.

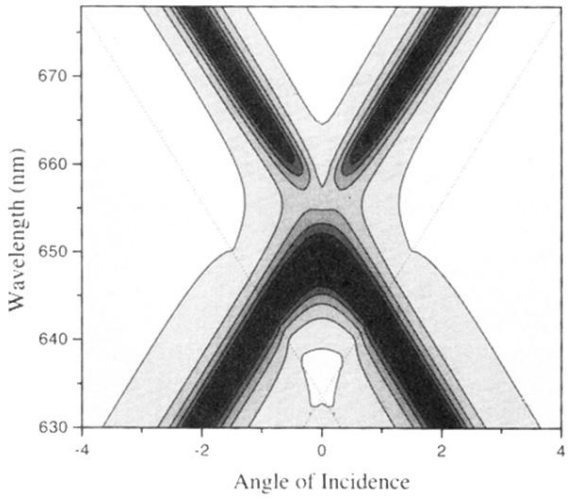

FIG. 7. Calculated reflectivity map for the grating exhibiting the energy gap. The dark regions correspond to low reflectivity, the light areas are high reflectivity. The dotted lines are the light lines representing the first order diffracted beams (see text).